

LA-UR-19-24824

Approved for public release; distribution is unlimited.

Title: Doppler Broadening Resonance Correction for Free-gas Scattering in MCNP6.2

Author(s): Brown, Forrest B.

Intended for: MCNP documentation
Report

Issued: 2019-05-23

Disclaimer:

Los Alamos National Laboratory, an affirmative action/equal opportunity employer, is operated by Triad National Security, LLC for the National Nuclear Security Administration of U.S. Department of Energy under contract 89233218CNA000001. By approving this article, the publisher recognizes that the U.S. Government retains nonexclusive, royalty-free license to publish or reproduce the published form of this contribution, or to allow others to do so, for U.S. Government purposes. Los Alamos National Laboratory requests that the publisher identify this article as work performed under the auspices of the U.S. Department of Energy. Los Alamos National Laboratory strongly supports academic freedom and a researcher's right to publish; as an institution, however, the Laboratory does not endorse the viewpoint of a publication or guarantee its technical correctness.

Doppler Broadening Resonance Correction for Free-gas Scattering in MCNP6.2

Forrest B. Brown

Monte Carlo Methods, Codes, & Applications (XCP-3), LANL
PO Box 1663, MS A143, Los Alamos, NM, 87544

ABSTRACT

The traditional treatment for epithermal neutron scattering in continuous-energy Monte Carlo codes is the free-gas scattering model with the scattering cross-section assumed constant in energy. Ouislomen and Sanchez demonstrated in 1991 that scattering resonances can cause significant departures from the free-gas model, and Becker proposed a correction to the Monte Carlo free-gas scattering model in 2009. Becker's Doppler Broadening Resonance Correction was tested in *mcnp5* in 2011 and recently implemented in *mcnp6.2*.

KEYWORDS: neutron transport, DBRC

1. INTRODUCTION

The traditional treatment for epithermal neutron scattering in continuous-energy Monte Carlo codes is the free-gas scattering model [1]. This model assumes that nuclide target motion follows a Maxwell-Boltzmann distribution of velocities and that the scattering cross-section is independent of energy. Typically, the free-gas model is used at epithermal energies up to 400 kT, and target-at-rest scattering is used at neutron higher energies. Scattering with hydrogen is a special case, with free-gas scattering used at all epithermal energies.

In 1991, Ouislomen and Sanchez [2] demonstrated that scattering resonances can have a significant effect on epithermal scattering, producing increased up-scattering compared to the free-gas model. The increased up-scattering, though small, results in increased capture in nearby capture resonances and noticeable decreases in k_{eff} . In 2009 Becker [3] proposed a straightforward modification to the free-gas scattering treatment that accounts for non-constant scattering cross-sections. Becker's method was tested in *mcnp5* in 2011 by Sunny and Brown [4,5], but not permanently implemented due to the absence of 0°K scattering data (which is required for Becker's method). Since the release of *mcnp6.1* in 2013 [6], 0°K nuclear data has been included with ENDF/B-VII.1 and ENDF/B-VIII.0 *mcnp* data libraries. In the current work, Becker's DBRC free-gas scattering was implemented as an optional feature in *mcnp6.2.1* [7,8].

2. METHODS

The collision physics and random sampling schemes used in *mcnp6* for conventional free-gas scattering have been thoroughly documented in [9,10]. The *mcnp5* implementation of Becker's DBRC method is documented in [4,5]. This report will summarize the key DBRC sampling modifications and focus on the new implementation of DBRC into *mcnp6.2.1*.

2.1. DBRC Modifications to Free-gas Sampling

Denoting v as the neutron velocity, V the target nuclide velocity, $\alpha = M_{target}/2kT$, and $P(V) = (\alpha/\pi)^{3/2} \exp(-\alpha V^2)$ as the Maxwellian target distribution, and constant scattering cross-section, then the Doppler broadened effective scattering cross-section is

$$\sigma_{eff,S}(v) = \sigma_S \left[\frac{e^{-\alpha v^2}}{v\sqrt{\pi\alpha}} + \left(1 + \frac{1}{2\alpha v^2}\right) \operatorname{erf}(v\sqrt{\alpha}) \right]$$

and the PDF (without DBRC) for selecting the target nuclide speed and cosine of the scattering angle is

$$P(V, \mu | v) dV d\mu = C [P_1 \cdot f_1(V) dV + P_2 \cdot f_2(V) dV] \cdot \frac{d\mu}{2} \cdot \frac{|\vec{v} - \vec{V}|}{v + V}$$

where

$$P_1 = \frac{v}{v + \frac{2}{\sqrt{\pi\alpha}}}, \quad f_1(V) = 4 \sqrt{\frac{\alpha^3}{\pi}} V^2 e^{-\alpha V^2}$$

$$P_2 = (1 - P_1), \quad f_2(V) = 2\alpha^2 V^3 e^{-\alpha V^2}$$

$$C = \sigma_S / \sigma_{eff,S}(v)$$

The Monte Carlo sampling scheme without DBRC is then:

- With probability P_1 sample V from $f_1(V)$, otherwise sample V from $f_2(V)$.
- Sample μ uniformly on $[-1,1]$.
- With probability $|\mathbf{v}\cdot\mathbf{V}| / (v+V)$, accept V and μ , and compute the exit neutron energy and scattering angle; otherwise reject V and μ , and resample.

Becker's DBRC method modifies the free-gas sampling scheme to:

$$P(V, \mu | v) dV d\mu = C' [P_1 \cdot f_1(V) dV + P_2 \cdot f_2(V) dV] \cdot \frac{d\mu}{2} \cdot \frac{|\vec{v} - \vec{V}|}{v + V} \cdot \frac{\sigma_S(v_{rel})}{\sigma_{max}(v)}$$

where $C' = \sigma_{max}(v) / \sigma_{eff,S}(v)$ and $v_{rel} = |\vec{v} - \vec{V}|$. The parameter $\sigma_{max}(v)$ is the largest 0°K scattering cross-section within $\pm 4/\sqrt{\alpha}$ of v .

The Monte Carlo sampling scheme with DBRC is then:

- With probability P_1 sample V from $f_1(V)$, otherwise sample V from $f_2(V)$.
- Sample μ uniformly on $[-1,1]$.
- With probability $|\mathbf{v}\cdot\mathbf{V}| / (v+V)$, accept V and μ , otherwise reject V and μ , and resample.
- With probability $\sigma_S(v_{rel}) / \sigma_{max}(v)$, accept V and μ , and compute the exit neutron energy and scattering angle; otherwise reject V and μ , and resample.

Thus, the DBRC modifications simply introduce an additional rejection test into the conventional free-gas sampling methods.

2.2. Modifications to MCNP6.2.1

2.2.1. **dbrc_make_lib** Utility Program

The **dbrc_make_lib** utility program was written to collect 0° K elastic scattering data for all nuclides from the ACE files for *mcnp6.2*, and to save those data in files to be stored in the \$DATAPATH directory for *mcnp6.2*. (The ACE data was actually generated at 0.1° K to avoid bugs in NJOY that occur for a temperature of exactly 0° K.) Two data files are created: `DBRC_endf71.txt` and `DBRC_endf80.txt`. The first file contains the energies and elastic scattering cross-sections for 424 nuclides from ACE files having the suffix “.85c,” corresponding to ENDF/B-VII.1 data at 0.1° K. The second contains the energies and elastic scattering cross-sections for 556 nuclides from ACE files having the suffix “.05c,” corresponding to ENDF/B-VIII.0 data at 0.1° K. By default, the data files are formatted ASCII text files. More compact binary files can be created if a code parameter is toggled. For each nuclide (designated by ZZZAAA without a suffix), the pairs of energy-scattering cross-section are stored over the energy range 1.0×10^{-5} eV through the first energy higher than 250.0 eV. (The upper limit could be raised by simply altering a program parameter.) The Fortran file format is simple:

```
(a80)      info - 80 characters of information about the data
(i8,es15.7) niso - number of nuclides,  emax - maximum energy covered (250 eV)
(10i8)     isos - list of ZZZAAA for all niso nuclides (no suffixes)
(10i8)     ne - list of number of energy/σs pairs for each nuclide
Repeat niso times:
(i8,i8)    ZZZAAA – nuclide identifier,  ne – number of energy/σs pairs
(6es13.6)  energies (ne entries)
(6es13.6)  elastic scattering cross-sections (ne entries)
```

Consolidating all of the 0° K elastic scattering data for all nuclides into a single file simplifies the process of retrieving this data during an *mcnp6.2* run. That is, only one compact data file needs to be read to obtain all required 0° K data, rather than many different ACE files. Creating the 2 datafiles takes only a few minutes. The file sizes are:

```
DBRC_endf71.txt - 38 MB
DBRC_endf80.txt - 48 MB
```

The **dbrc_make_lib** utility program was added to the *mcnp6* git repository (for *mcnp6.2.1*) branch `features/DBRC` in the directory `mcnp6/Utilities/DBRC_LIB`.

2.2.2. DBRC Input Card for *mcnp6.2*

The DBRC input card was created to provide user control over the DBRC treatment.

If the DBRC card is not present among the *mcnp6.2* data cards, then the traditional MCNP free-gas scattering treatment is used, with free-gas scattering for 1-H-1 at all energies and free-gas scattering at energies below 400 kT for all other nuclides (for energies higher than the range of $S(\alpha,\beta)$ data if used for a nuclide).

If the DBRC card is present among the *mcnp6.2* data cards, then the following format and options are available:

DBRC	[endf= nn]	[emax= eee]	[isos= iso_list]
endf= nn	<i>nn</i> must be either 71 or 80, for selecting either ENDF/B-VII.1 or ENDF/B-VIII.0 scattering data at 0° K. Note that the at 0° K data must be entirely ENDF/B-VII.1 or ENDF/B-VIII.0, and not a mix of the 2. This entry is required if 1 or more nuclides are listed in the <i>iso_list</i> .		
emax= eee	<i>eee</i> is the upper energy limit for applying DBRC for all nuclides except 1-H-1, in units of MeV. The default is 2.1×10^{-6} MeV (210 eV). Note that the <i>eee</i> limit applies to all nuclides except 1-H-1, even those not listed in the <i>iso_list</i> . If <i>eee</i> is specified and the <i>iso_list</i> is not present, then conventional free-gas scattering is performed for all nuclides up to <i>eee</i> , rather than the traditional 400 kT limit. <i>eee</i> must be less than or equal to the DBRC_endf71 or DBRC_end80 datafile upper limit, currently 250 eV.		
isos= iso_list	<i>iso_list</i> is a list of 1 or more ZZZAAA numbers, without suffixes. DBRC will be used for all nuclides in the list. If the <i>iso_list</i> is absent, then <i>emax=eee</i> may be used to directly set the upper limit for conventional free-gas scattering for all nuclides other than 1-H-1.		

DBRC card examples:

- Use DBRC for U-238, ENDF/B-VII.1, default energy cutoff 210 eV:

```
DBRC   endf=71   isos= 92238
```

- Use DBRC for U-234, u-235, U-236, U-238, ENDF/B-VIII.0, energy cutoff 230 eV:

```
DBRC   endf=80   emax=230.e-6   isos= 92234 92235 92236 92238
```

- Set the upper energy cutoff to 210 eV for free-gas scatter, without using DBRC for any isotopes:

```
DBRC   emax= 2.10e-6
```

To support the DBRC card, a number of source files were modified: *imcn.F90*, *mcnp_input.F90*, *mcnp_options.F90*, *nextit.F90*, *nxttit1.F90*.

A few supporting routines were modified for reading cross-section data, reading/writing the runtpe file, and MPI data transfers: *xact.F90*, *tpefil.F90*, *msgcon.F90*, *msgtsk.F90*.

All of the modified files were added to the *mcnp6* git repository (for *mcnp6.2.1*) branch *features/DBRC* in the directory *mcnp6/Source/src*.

2.2.3. `dbrc_scatter.F90` Module

This module contains 2 functions called during neutron collision physics (`sig0k_max` and `sig0k`) and 7 subroutines used by the input setup and support routines listed at the end of Section 2.2.2. For collisions with nuclides listed on the DBRC card, `sig0k_max` is called before the free-gas scattering rejection loop in `tgtvel.F90` to obtain the maximum 0° K elastic scattering cross-section in the neighborhood of the incoming neutron energy. `sig0k` is called in `tgtvel.F90` as part of an outer rejection loop.

Data from the `dbrc_scatter.F90` module is used in several routines to determine whether to call the `tgtvel` routine: `colidn.F90`, `tallyd.F90`. The modified files and the new `dbrc_scatter.F90` file were added to the *mcnp6* git repository (for *mcnp6.2.1*) branch `features/DBRC` in the directory `mcnp6/Source/src`.

3. TESTING

Results from *mcnp6.2.1* using DBRC were principally compared with results from the previous implementation of DBRC in *mcnp5* as reported in [4,5]. In [4,5], *mcnp5* DBRC results were compared with results from [13,14], and a later work [15] compared results with those cited in [4.5]. In addition, [4,5] made detailed studies of the double-differential scattering kernel exit energy distributions.

It should be noted that verification results reported in [4,5] were based on the ENDF/B-VII.0 data available at the time, whereas the present results were obtained using ENDF/B-VII.1 data. Differences in the nuclear data are very minor.

3.1. Double-differential Scattering Kernels

Figure 1 shows the exit energy distributions obtained with and without DBRC using *mcnp6.2.1* for 92-U-238 elastic scattering at 1200° K for an incident neutron energy of 6.52 eV. The plot shows exactly the same behavior as Figure 5 from [4]. DBRC significantly increases the upscattering as expected.

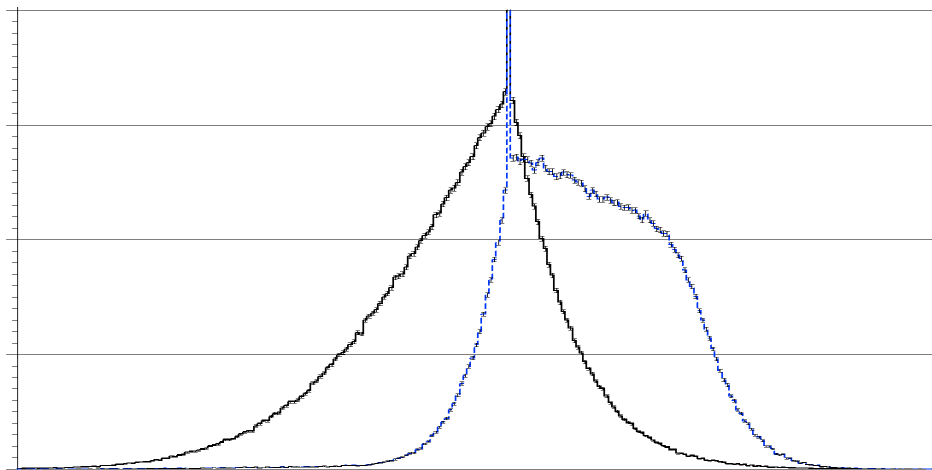


Figure 1. Comparison of exit energy distributions for 6.52 eV neutron incident on 92-U-238 at 1200° K, with DBRC (blue) and without DBRC (black), plot range [6 eV, 7 eV]

3.2. Mosteller Doppler Defect Benchmark Problem

The Mosteller benchmark problem [11,12] for LWR pin cell with UO₂ fuel was used in [4,5] to benchmark *mcnp5* results using ENDF/B-VII.0 nuclear data with resonance scattering to the results published in [13,14]. The current implementation of DBRC in *mcnp6.2.1* uses ENDF/B-VII.1 nuclear data. Figure 2 shows the basic geometry used for all cases.

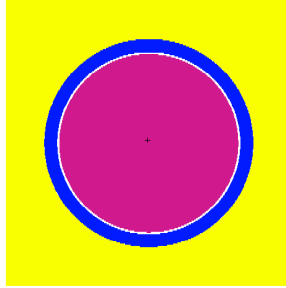


Figure 2. LWR Pin Cell in Mosteller Benchmark [11]

In order to calculate the Fuel Temperature Coefficient (FTC), two sets of calculations are done in *mcnp*. The first is at Hot Zero Power (HZP) conditions where the fuel, cladding and moderator are set at a temperature of 600° K. The second set of calculations is done under Hot Full Power (HFP) conditions where the fuel temperature is set at 900° K and the cladding and moderator temperatures are at 600° K. The calculations were done for 7 fuel enrichments (weight%): 0.711, 1.6, 2.4, 3.1, 3.9, 4.5, 5.0.

The FTC in units of pcm/°K is calculated from:

$$FTC = \frac{\rho_{HFP} - \rho_{HZP}}{\Delta T} \cdot 10^5 = \left(\frac{1}{k_{HZP}} - \frac{1}{k_{HFP}} \right) \cdot \frac{10^5}{\Delta T}$$

Table 1 presents the results for the Mosteller benchmark **without using DBRC** for *mcnp5* using ENDF/B-VII.0 data (2011) and *mcnp6.2.1* using ENDF/B-VII.1 data (2019). That is, the standard, traditional *mcnp* free-gas model is used at all energies for 1-H-1 and up to 400 kT for all other nuclides. Differences between the 2011 and 2019 results are due to small differences in the codes, to Monte Carlo statistics, and to minor differences between the ENDF/B data. Most results between 2011 and 2019 agree within 1 σ , and all agree within 2 σ .

Table 2 presents the results for the Mosteller benchmark **using DBRC** for *mcnp5* using ENDF/B-VII.0 data (2011) and *mcnp6.2.1* using ENDF/B-VII.1 data (2019). It should be noted that the results in Table 2 may have small differences due to a different treatment of the energy cutoff for free-gas scattering. In the 2011 work with *mcnp5*, nuclides that did not use DBRC used the free-gas scattering energy cutoff of 400 kT. In the 2019 work using *mcnp6.2.1*, all nuclides – using DBRC or not – used the free-gas scattering energy cutoff of 210 MeV. Differences between the 2011 and 2019 results are due to small differences in the codes, to Monte Carlo statistics, and to minor differences between the ENDF/B data. Most results between 2011 and 2019 agree within 1 σ , and all agree within 2 σ .

Table 3 summarizes the change in FTC due to the DBRC treatment, comparing the effect seen with *mcnp5* using ENDF/B-VII.0 data (2011) and *mcnp6.2.1* using ENDF/B-VII.1 data (2019). There is more variability in the comparisons since the changes are differences in differences of results. All of the differences in the FTCs agree within 1σ for the *mcnp5* runs in 2011 and the *mcnp6* runs in 2019.

Figure 3 shows the FTC results for the Mosteller benchmark using *mcnp5* from 2011 and *mcnp6* from 2019.

Table 1. Comparison of results for Mosteller problem using standard *mcnp5* (2011) and *mcnp6.2.1* (2019), without DBRC

MCNP WITHOUT DBRC								
	<i>mcnp5</i> , 2011			<i>mcnp6.2</i> , 2019			Difference, <i>mcnp6</i> – <i>mcnp5</i>	
wt%	HZP			HZP				
0.711	0.66569	±	0.00019	0.66577	±	0.00006	0.00008	± 0.00020
1.6	0.96124	±	0.00026	0.96091	±	0.00008	-0.00033	± 0.00027
2.4	1.09913	±	0.00026	1.09911	±	0.00009	-0.00002	± 0.00028
3.1	1.17657	±	0.00030	1.17705	±	0.00009	0.00048	± 0.00031
3.9	1.23944	±	0.00028	1.23957	±	0.00010	0.00013	± 0.00030
4.5	1.27495	±	0.00032	1.27510	±	0.00009	0.00015	± 0.00033
5.0	1.29920	±	0.00034	1.29937	±	0.00009	0.00017	± 0.00035
wt%	HFP			HFP				
0.711	0.65987	±	0.00020	0.65984	±	0.00006	-0.00003	± 0.00021
1.6	0.95295	±	0.00025	0.95277	±	0.00008	-0.00018	± 0.00026
2.4	1.08986	±	0.00029	1.08997	±	0.00009	0.00011	± 0.00030
3.1	1.16777	±	0.00027	1.16759	±	0.00009	-0.00018	± 0.00028
3.9	1.23009	±	0.00027	1.22974	±	0.00009	-0.00035	± 0.00028
4.5	1.26542	±	0.00027	1.26486	±	0.00009	-0.00056	± 0.00028
5.0	1.28911	±	0.00029	1.28927	±	0.00009	0.00016	± 0.00030
wt%	FTC (pcm/K)			FTC (pcm/K)				
0.711	-4.42	±	0.21	-4.50	±	0.06	-0.08	± 0.22
1.6	-3.02	±	0.13	-2.96	±	0.04	0.05	± 0.14
2.4	-2.58	±	0.11	-2.54	±	0.04	0.04	± 0.11
3.1	-2.13	±	0.10	-2.29	±	0.03	-0.16	± 0.10
3.9	-2.04	±	0.09	-2.15	±	0.03	-0.11	± 0.09
4.5	-1.97	±	0.09	-2.12	±	0.03	-0.15	± 0.09
5.0	-2.01	±	0.09	-2.01	±	0.03	-0.00	± 0.09

Table 2. Comparison of results for Mosteller problem using standard *mcnp5* (2011) and *mcnp6.2.1* (2019), with DBRC

MCNP WITH DBRC								
	<i>mcnp5</i> , 2011			<i>mcnp6.2</i> , 2019			Difference, <i>mcnp6</i> – <i>mcnp5</i>	
wt%	HZP			HZP				
0.711	0.66541	±	0.00022	0.66541	±	0.00006	0.00000	± 0.00023
1.6	0.96044	±	0.00026	0.96049	±	0.00008	0.00005	± 0.00027
2.4	1.09889	±	0.00027	1.09866	±	0.00009	-0.00023	± 0.00028
3.1	1.17613	±	0.00026	1.17638	±	0.00009	0.00025	± 0.00028
3.9	1.23924	±	0.00029	1.23906	±	0.00009	-0.00018	± 0.00030
4.5	1.27460	±	0.00025	1.27448	±	0.00009	-0.00012	± 0.00027
5.0	1.29860	±	0.00029	1.29870	±	0.00009	0.00010	± 0.00031
wt%	HFP			HFP				
0.711	0.65909	±	0.00020	0.65908	±	0.00006	-0.00001	± 0.00021
1.6	0.95142	±	0.00022	0.95143	±	0.00008	0.00001	± 0.00023
2.4	1.08877	±	0.00029	1.08826	±	0.00008	-0.00051	± 0.00030
3.1	1.16563	±	0.00028	1.16583	±	0.00009	0.00020	± 0.00029
3.9	1.22866	±	0.00030	1.22796	±	0.00009	-0.00070	± 0.00031
4.5	1.26271	±	0.00031	1.26319	±	0.00009	0.00048	± 0.00032
5.0	1.28748	±	0.00030	1.28733	±	0.00009	-0.00015	± 0.00031
wt%	FTC (pcm/K)			FTC (pcm/K)				
0.711	-4.80	±	0.23	-4.81	±	0.06	-0.01	± 0.24
1.6	-3.29	±	0.12	-3.30	±	0.04	-0.01	± 0.13
2.4	-2.82	±	0.11	-2.90	±	0.03	-0.08	± 0.12
3.1	-2.55	±	0.09	-2.56	±	0.03	-0.01	± 0.10
3.9	-2.32	±	0.09	-2.43	±	0.03	-0.12	± 0.10
4.5	-2.46	±	0.08	-2.34	±	0.03	0.12	± 0.09
5.0	-2.22	±	0.08	-2.27	±	0.03	-0.05	± 0.09

Table 3. Comparison of Using DBRC with No DBRC, for mcnp5 (2011) and mcnp6.2.1 (2019)

DIFFERENCE IN FTC (DBRC – standard)/standard				
	<i>mcnp5</i> , 2011		<i>mcnp6.2.1</i> , 2019	
wt%	FTC Diff (%)	Error (%)	FTC Diff (%)	Error (%)
0.711	-8.8	7.0	-6.9	2.0
1.6	-9.1	6.0	-11.5	2.0
2.4	-9.3	6.0	-14.0	1.9
3.1	-19.6	6.3	-11.8	1.9
3.9	-13.3	6.1	-13.1	1.9
4.5	-25.1	6.1	-10.5	1.8
5.0	-10.4	6.1	-12.8	1.8

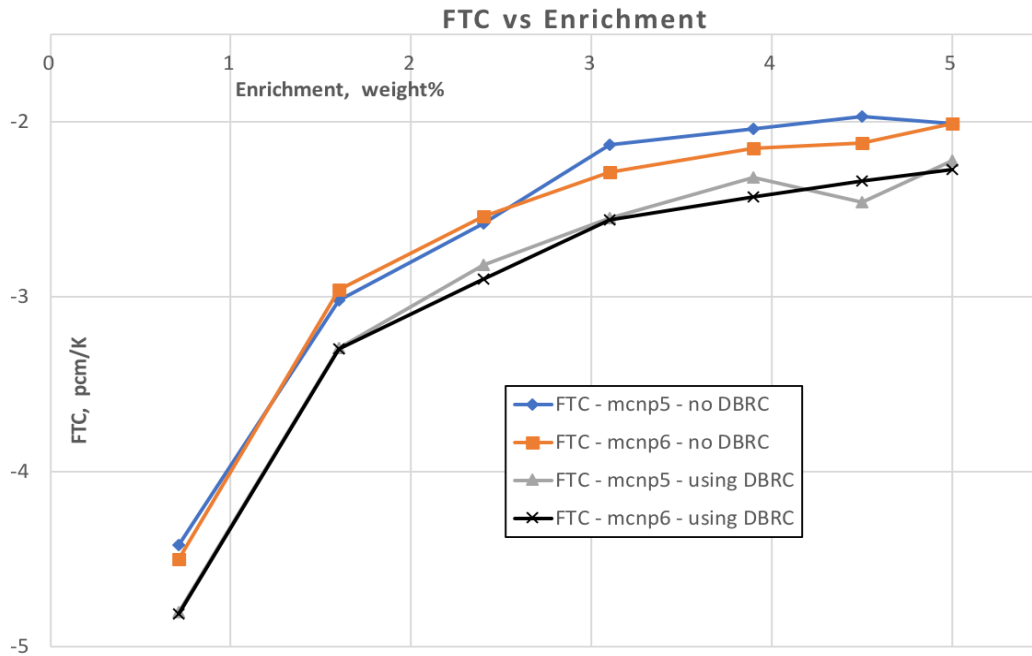


Figure 3. FTC Results for the Mosteller Doppler Defect Benchmark

4. CONCLUSIONS

This report documents the recent work to implement the Doppler Broadening Resonance Correction to free-gas scattering into *mcnp6.2.1*. The code algorithms and basic DBRC method were previously detailed in [4,5], and testing/verification was performed in 2011 using *mcnp5*, the ENDF/B-VII.0 nuclear data, and the specific nuclide 92-U-238. The present work extends the previous DBRC feature, with general capabilities to do any or all nuclides, to vary the upper energy cutoff for DBRC and free-gas scatter, and to use 0° K elastic scattering data for any isotope in either the ENDF/B-VII.1 or ENDF/B-VIII.0 nuclear data libraries.

Care was taken to ensure that the coding for the current implementation of DBRC into *mcnp6.2.1* is efficient. While the previous 2011 *mcnp5* DBRC was 5-15% slower than standard *mcnp5*, the DBRC implementation in *mcnp6.2.1* is only 0-5% slower than the standard *mcnp6.2.1*.

The new DBRC implementation into *mcnp6.2.1* was tested by comparison with results from 2011 for the Mosteller benchmark for the Doppler defect. Results agree very well, with most results agreeing within 1σ , and all agreeing within 2σ . Examination of the detailed exit energy distribution with and without DBRC has also verified that the new implementation is correct.

5. AVAILABILITY

The *mcnp6.2.1* code modifications to support DBRC are stored in
LANL XCP-3 git repository: **mcnp6**
Branch: **features/DBRC**

This branch is kept in sync with the main *mcnp6.2* development branch, **mcnp6_devel**.

The **features/DBRC** branch will be merged into the **mcnp6_devel** branch during summer 2019, and will be included in the next version of *mcnp6* that is distributed through RSICC.

The version of *mcnp6.2.1* with DBRC will be available by special request to staff at DOE laboratories who have already obtained an *mcnp6* license from RSICC. Interested researchers should directly contact F. B. Brown by email, fbrown@lanl.gov, to make arrangements.

ACKNOWLEDGMENTS

This work was supported by the US DOE Consortium for Advanced Simulation of LWRs (CASL).

REFERENCES

Note: LANL reports cited below are available in the MCNP Reference Collection on the MCNP web site, mcnp.lanl.gov.

1. R.R. Coveyou, R.R. Bate, R.K. Osborn, "Effect of Moderator Temperature upon Neutron Flux in Infinite Capturing Medium", *J. Nuclear Energy*, Vol. 2, pp153-167 (1956).
2. M. Ouisloumen, R. Sanchez, "A model for neutron scattering off heavy isotopes that accounts for thermal agitation effects", *Nucl. Sci. Eng.* **107**, 189–200 (1991).

3. B. Becker, R. Dagan & G. Lohnert, "Proof and implementation of the stochastic formula for ideal gas, energy dependent scattering kernel," *Annals of Nuclear Energy*, **36**, pp. 470 – 474 (2009).
4. E.E. Sunny, F.B. Brown, B.C. Kiedrowski, W.R. Martin, "Temperature Effects of Resonance Scattering in Free Gas for Epithermal Neutrons", LANL report LA-UR-11-04886 (2011).
5. E.E. Sunny, F.B. Brown, B.C. Kiedrowski, W.R. Martin, "Temperature Effects of Resonance Scattering for Epithermal Neutrons in MCNP", ANS PHYSOR-2012, Knoxville TN, 15-20 April, also LANL report LA-UR-11-06503 (2011).
6. T. Goorley, et al., "Initial MCNP6 Release Overview", *Nuclear Technology*, **180**, pp 298-315 (2012).
7. C.J. Werner, et al., "MCNP6.2 Release Notes", LANL report LA-UR-18-20808 (2018).
8. J.C. Armstrong, "MCNP6.2.1 Release Notes", LANL report LA-UR-18-31546 (2018).
9. X-5 Monte Carlo Team, "MCNP - Version 5, Vol. I: Overview and Theory", pages 2-28 through 2-31, LANL report LA-UR-03-1987 (2003).
10. L.L. Carter and E.D. Cashwell, Particle Transport Simulation with the Monte Carlo Method, ERDA Critical Review Series, TID-26607, National Technical Information Service, Springfield MA (1975).
11. R. D. Mosteller, "Computational Benchmarks for the Doppler Reactivity Defect," LA-UR-06-2968, Los Alamos National Laboratory.
12. R. D. Mosteller, "ENDF/B-V, ENDF/B-VI, and ENDF/B-VII.0 Results for the Doppler-defect Benchmark," Proceedings from M&C+SNA, Monterey, CA (2007).
13. D. Lee, K. Smith & J. Rhodes, "The impact of ^{238}U resonance elastic scattering approximations on thermal reactor Doppler reactivity," *Annals of Nuclear Energy*, **36**, pp. 274-280 (2009).
14. T. Mori & Y. Nagaya, "Comparison of Resonance Elastic Scattering Models Newly Implemented in MVP Continuous-Energy Monte Carlo Code," *Journal of Nuclear Science and Technology*, Vol 46, No. 8, pp. 793- 798 (2009).
15. J.A. Walsh, B. Forget, K.S. Smith, "Accelerated Sampling of the Free-Gass Resonance Elastic Scattering Kernel", *Annals of Nuclear Energy*, **69**, 116-124 (2014).